DWT based bearing fault detection in induction motor using noise cancellation

K.C. Deekshit Kompella [a,*], Venu Gopala Rao Mannam [b], Srinivasa Rao Rayapudi [c]

[a] *Department of Electrical & Electronics Engineering, K L University, Guntur, A.P., India*
[b] *Department of Electrical & Electronics Engineering, PVPSIT, Kanuru, A.P., India*
[c] *Department of Electrical & Electronics Engineering, JNTUK, Kakinada, A.P., India*

Abstract

This paper presents an approach to detect the bearing faults experienced by induction machine using motor current signature analysis (MCSA). At the incipient stage of bearing fault, the current signature analysis has shown poor performance due to domination of pre fault components in the stator current. Therefore, in this paper domination of pre fault components is suppressed using noise cancellation by Wiener filter. The spectral analysis is carried out using discrete wavelet transform (DWT). The fault severity is estimated by calculating fault indexing parameter of wavelet coefficients. It is further proposed that, the fault indexing parameter of power spectral density (PSD) based wavelet coefficients gives better results. The proposed method is examined using simulation and experiment on 2.2 kW test bed.
© 2016 Electronics Research Institute (ERI). Production and hosting by Elsevier B.V. This is an open access article under the CC BY-NC-ND license (http://creativecommons.org/licenses/by-nc-nd/4.0/).

Keywords: Fault detection; Motor current signature analysis (MCSA); Discrete wavelet transforms (DWT); Power spectral density; Wiener filter
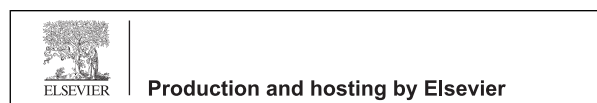
1. Introduction

Most of the industries depend on squirrel cage induction motors, due to its stalwart structure, high power to weight ratio, high reliability and easy design. Even though these motors are rugged in structure, they often face many faults, if they are operating for a long time without monitoring (Report, 1985a,b). Among the faults experienced by induction motors, bearing faults contribute to 41% in a 200 hp motor as shown in Fig. 1 (Soualhi et al., 2015; Zhang et al., 2011). The contribution of bearing fault may vary from 40% to 90% in large to small range machines (El Houssin et al., 2013). As these faults become severe, there may be unexpected interruption of industrial process. To prevent this unexpected damage, it is essential to predict these faults at nascent stage. Conventionally vibrating sensors are used to monitor these

---

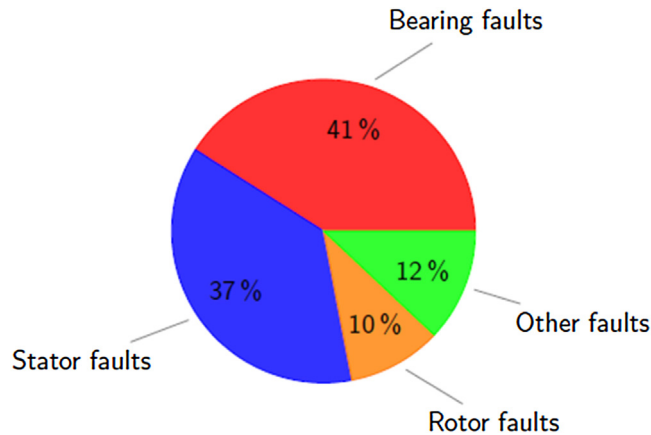**Production and hosting by Elsevier**

Fig. 1. Pie diagram of faults experienced by induction motor.

faults, which are costly and suitable to large range machines only (Blodt et al., 2008). In contrast to this, the current signature analysis has overcome these drawbacks and gives good performance even in noisy atmosphere (Eren and Devaney, 2004; Stack et al., 2004a; Filippetti et al., 1995; Obaid et al., 2003; Bellini et al., 2008a). These advantages of motor current signature analysis (MCSA) have attracted many researchers in the last few years. Conventional current spectral analysis using FFT has many draw backs like spectral leakage, poor resolution and disables to provide time frequency relation etc. To overcome the drawbacks in FFT, window functions are commonly employed (Jung et al., 2006; Liu et al., 2008) in spectral analysis. Fault detection using time–frequency techniques, such as short-time Fourier transform (STFT) (Kim et al., 2007), the Wigner–Ville distribution (WVD) (Vicente et al., 2014; Kim et al., 2007) have few drawbacks like the STFT uses fixed windows for all frequencies which gives poor resolution and WVD is complex due to cross terms. To overcome these drawbacks in time–frequency analysis, the wavelet transform (WT) based fault detection is presented in Lau and Ngan (2010), Sun et al. (2013), Luo et al. (2013) and Wei et al. (2011).

Based on the location of fault, bearing defects can be classified into two types: (1) single point defect (Cyclic) and (2) generalized roughness (Non Cyclic). Further, the single point defect can be sub classified as (a) outer race faults, (b) inner race fault, (c) ball defect and (d) cage fault (Frosini and Bassi, 2010). These cyclic faults will generate detectable vibrations by producing an impact between the ball and raceway. The characteristic vibrating frequencies due to these faults can be calculated using Eqs. (1)–(4), (Frosini and Bassi, 2010).

The vibration frequency due to outer race fault, f_{out} is given by

$$f_{out} = \frac{n}{2} f_r \left(1 - \frac{BD}{PD} \cos\emptyset \right) \tag{1}$$

The vibration frequency due to inner race fault, f_{inn} is given by

$$f_{inn} = \frac{n}{2} f_r \left(1 + \frac{BD}{PD} \cos\emptyset \right) \tag{2}$$

The vibration frequency due to ball defect, f_{ball} is given by

$$f_{ball} = \frac{PD}{2BD} f_r \left(1 - \left(\frac{BD}{PD} \right)^2 \cos^2\emptyset \right) \tag{3}$$

The vibration frequency due to cage fault, f_{cage} is given by

$$f_{cage} = \frac{1}{2} f_r \left(1 - \frac{BD}{PD} \cos\emptyset \right) \tag{4}$$

Where n is the number of balls, $\emptyset$ is the contact angle, PD is the pitch diameter, BD is the ball diameter of the bearing, and f_r is the rotor speed in Hz as shown in Fig. 2.
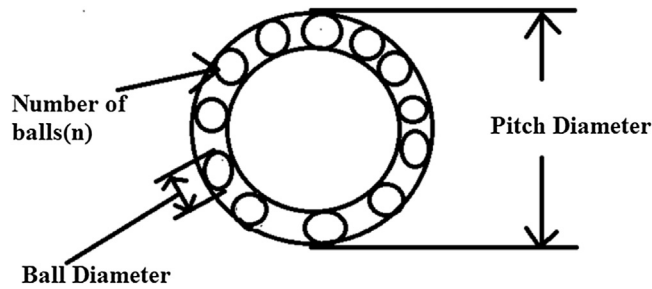
Fig. 2. Geometry of bearing.

These vibrating frequencies due to bearing defect will reflect in to the stator current spectrum by affecting the air gap flux density (Obaid et al., 2003). The fault frequencies in stator current can be calculated from vibrating frequencies and fundamental component using following equation.

$$f_{\text{bearing}} = |f_s \pm m.f_v| \tag{5}$$

where $m = 1, 2, 3. . .$, f_{bearing} is the characteristic fault frequency in stator current, f_s is the fundamental frequency and f_v is the vibration frequency for different faults.

Similarly, the generalized roughness faults can be classified into (a) deformation of the seal and (b) corrosion (Frosini and Bassi, 2010). The prediction of generalized roughness faults is difficult, because they are not visible to unaided eye and they may not produce characteristic fault frequencies in both vibration and stator current (Schoen et al., 1995; Stack et al., 2004c).

Many of the researchers (Sun et al., 2013; Luo et al., 2013; Wei et al., 2011; Schoen et al., 1995; Stack et al., 2006; Zhongming et al., 2001; Bellini et al., 2008b; Kia et al., 2007; Garcia-Perez et al., 2011; Kim et al., 2013) have concentrated on the fault location and severity, which are suitable to first category of the fault i.e. single point defect. On the other hand the detection of generalized faults is a challenging task to the researchers due to their progressive nature. Even though the estimation of generalized faults presented in Stack et al. (2004b), Zhou et al. (2009), Kompella et al. (2013) and El Houssin et al. (2013) have few drawbacks. For example in Stack et al. (2004b), it requires detailed knowledge about spectral distribution, harmonics and eccentricity etc. In Zhou et al. (2009), the generalized roughness faults can be detected by cancelling the healthy components and the fault can be estimated by RMS value of noise cancelled stator current. But the authors do not discuss the fault analysis and its classification under the presence of noise. The fault classification and analysis is carried out using FFT in Kompella et al. (2013) has noise problems and fault component is suppressed by noise especially at early stage. In El Houssin et al. (2013) discrete wavelet transform (DWT) analysis is presented with frequency subtraction, it does not give good results due to spectral subtraction is performed without any filter.

In contrast to these, this paper presents the detection of bearing faults using noise cancellation with DWT analysis by an adaptive filter (Wiener filter). The domination of pre fault components in the stator current is suppressed by cancelling them in a real time fashion using Wiener filter. To improve the resolution, the spectral analysis of stator current after noise cancellation is carried out using DWT. In addition to this, the fault severity can be estimated using statistical parameters namely standard deviation (SD) and energy of wavelet coefficients as fault indexing parameters. To elevate the fault index parameters for better indication, the power spectral density of wavelet coefficients is presented.

2. System modeling

The block diagram of proposed bearing fault detection topology is shown in Fig. 3. In the first stage, the stator current under healthy and faulty conditions of bearing is attained using current transducer and processed by data acquisition system. In the second stage, acquired stator current processed for noise cancellation using Wiener filter to suppress the domination of pre fault components. Afterwards, the noise cancelled stator current is decomposed using DWT in to sufficient levels depending on sampling frequency, rated speed etc. In the next stage the power spectral density (PSD) of wavelet coefficients is calculated and is used to estimate the fault severity. In last stage of fault detection, the statistical parameters SD and energy are calculated to indicate the fault severity.

Fig. 3. Block diagram of proposed bearing fault detection topology.

2.1. Noise cancellation

Under healthy conditions (with respect to bearing defect) of induction machine, the stator current usually consist the fundamental component, harmonics, and the noise components (sensors and EMI) (Zhou et al., 2009). These components will remain even after the bearing fault exists and may dominate the fault component at incipient stage. Therefore, the healthy components in the stator current is predicted and cancelled in a real time fashion using Wiener filter. The design of Wiener filter is described in the following. The mathematical model of stator current is given by

$$x(n) = x_0(n) + \sum_{h=0}^{M} A_k \sin(h\omega_0 n) + x_n(n) \tag{6}$$

where
$x_0(n)$ fundamental component
$x_n(n)$ noise component due to sensors and EMI
ω_0 fundamental frequency
h order of the harmonic component
$b(n)$ bearing fault component
$X_f(n)$ Stator current with bearing fault
n_0 number of delay units
P order of the Wiener filter
$W(z)$ Wiener filter
Whenever bearing fault develops, a fault component will be added in the stator current and the Eq. (6) becomes

$$x_f(n) = x(n) + b(n) \tag{7}$$

where $b(n)$ is bearing fault component and is estimated by eliminating the healthy components of the motor current. Simple subtraction of the healthy component from the faulty current (El Houssin et al., 2013) will not give good performance due to random nature of the noise. Therefore, in this paper the healthy components of the stator current are treated as noise and are cancelled in a real time fashion by using an adaptive filter (Wiener filter). The process of noise cancellation using Wiener filter is shown in Fig. 4 and is redrawn in Fig. 5.
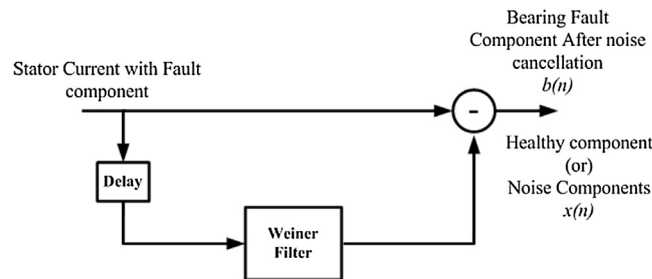

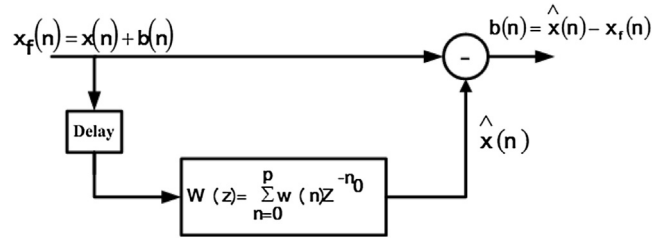Fig. 4. Stator current noise cancellation.

Fig. 5. Wiener filter based noise cancellation.

2.2. Filter design

In this section, the design of Wiener filter in Zhou et al. (2009) has been adopted to obtain the coefficients of the filter. The filter coefficients are designed in minimum mean square sense to minimize the prediction error ξ. This error occurs because of the deviation of estimated components from original components of the stator current. The filter is said to be ideal, if the predicted components are same as the original components under healthy conditions of the bearing. i.e. $\hat{x}(n) \approx x(n)$. The predicted components of noise is given by

$$\hat{x}(n) = \sum_{k=0}^{p} w(k) x_f(n - n_0 - k) \tag{8}$$

where p is the order of the filter and n_0 is the number of delay units. The prediction error is given by

$$e(n) = |x(n) - \hat{x}(n)| \tag{9}$$

Then the mean square error from Eqs. (8) and (9) is given by

$$\xi = E\left\{e(n)e^*(n)\right\} = E\left\{|e(n)|^2\right\} \tag{10}$$

$$\xi = E\left\{|e(n)|^2\right\} = E\left\{|x(n) - \sum_{k=0}^{p} w(k) x_f(n - n_0 - k)|^2\right\} \tag{11}$$

where $E\{.\}$ stands for expectation. To minimize the prediction error in Eq. (11), differentiate ξ with respect to $w(k)$ and equating to zero. Then

$$\frac{\partial \xi}{\partial w(k)} = E\left\{2e(n)\frac{\partial e(n)}{\partial w(k)}\right\} = 0 \tag{12}$$

BysimplifyingtheEq.(12)

$$E\left\{e(n) x(n - n_0 - k)\right\} = 0, \quad k = 0, 1, \ldots p \tag{13}$$

This is known as *principle of orthogonality* and can be modified as follows

$$E\left\{\left[x(n) - \sum_{j=0}^{p} w(j) x(n - n_0 - j)\right] x(n - n_0 - k)\right\} = 0 \tag{14}$$

Since signal $x(n)$ is assumed to be wide-sense stationary, the auto correlation sequence of $x(n)$ is given by

$$\sum_{j=0}^{p} w(j) r_x(k - j) = r_x(n_0 + k), \quad k = 0, 1, 2, \ldots p \tag{15}$$

In matrix form, (15) can be written as

$$
\begin{bmatrix}
r_x(0) & r_x(1) & \cdots & r_x(p) \\
r_x(1) & r_x(0) & \cdots & r_x(p-1) \\
\vdots & \vdots & & \vdots \\
r_x(p) & r_x(p-1) & \cdots & r_x(0)
\end{bmatrix}
\begin{bmatrix}
w(0) \\
w(1) \\
\vdots \\
w(p)
\end{bmatrix}
=
\begin{bmatrix}
r_x(n_0) \\
r_x(n_0+1) \\
\vdots \\
r_x(n_0+p)
\end{bmatrix}
\tag{16}
$$

Eq. (6) may be written more briefly as

$$
R_x W = r_{dx} \tag{17}
$$

where R_x is a auto correlation matrix, W is the filter coefficients and r_{dx} cross correlation matrix between desired signal and the observed signal.

The filter coefficients can be obtained as

$$
W = R_x^{-1} r_{dx} \tag{18}
$$

2.3. Fault estimation

Whenever bearing fault develops, prediction capability of the filter decreases. Then the prediction error after noise cancellation will increase and the bearing fault frequency can be easily extracted from the stator current as given below.

$$
b(n) = x(n) - \sum_{k=0}^{p} w(k) x_f(n - n_0 - k) \tag{19}
$$

Under the healthy condition of the bearing the Eq. (19) has minimum value due to prediction error and will increase as the bearing fault develops. This value becomes high, if severe fault occurs. Especially at the nascent stage of fault, this value is very low and almost equal to healthy condition due to prediction error in the filter design. At this stage extraction of fault component from stator current is very difficult. Therefore the spectral analysis of stator current after noise cancellation is presented in the following subsection. After evaluating the fault component from (19), frequency analysis can be done in two ways.

2.3.1. FFT

The FFT analysis of bearing fault component will give the complete details of the fault like frequency response and magnitude response. The FFT analysis can be done using below expression.

$$
B(\omega) = \sum_{n=0}^{N-1} b(n) e^{-j\omega n} \tag{20}
$$

where N is the length of the signal $b(n)$ and $\omega = 2\pi mn/N$, $m = 0, 1, \ldots N-1$.

2.3.2. DWT

The bearing fault signal $b(n)$ can be expressed as approximation coefficients and detail coefficients using DWT, which represents low and high frequency components respectively (Hedayati Kia et al., 2009). In this work, Daubechies wavelet is taken to calculate the approximation and detail coefficients in each level using below expressions (Hedayati Kia et al., 2009).

$$
A_1(m) = \sum_{n} L(n - 2m) b(n) \tag{21}
$$

$$
D_1(m) = \sum_{n} H(n - 2m) b(n) \tag{22}
$$

Table 1
Machine details.

S. no.	Name plate detail	Rating
1	Power rating	2.2 kW
2	Rated speed	1435–1500 rpm
3	Rated voltage	415 V
4	Rated current	4.4 A

where A_1, D_1 are the approximate and detail coefficients at level 1 and L, H are the low and high pass filters respectively. The approximation and details coefficients at next level can be obtained using A_1, D_1 from the below equations.

$$A_2(m) = \sum_n L(n - 2m) A_1(n) \tag{23}$$

$$D_2(m) = \sum_n H(n - 2m) D_1(n) \tag{24}$$

Similarly the jth level coefficients can be obtained from $j - 1$th level coefficients as below.

$$A_j(m) = \sum_n L(n - 2m) A_{j-1}(n) \tag{25}$$

$$D_j(m) = \sum_n H(n - 2m) D_{j-1}(n) \tag{26}$$

The decomposition level j can be obtained by using

$$j = \text{integer} \left[\frac{\ln\left(\frac{F_s}{8 s_r f}\right)}{\ln 2} - 1 \right] \tag{27}$$

where s_r is slip and f is the fundamental component. After computing the jth level coefficients, fault estimation criteria can be done using two parameters. These criteria are the ratio of standard deviation of faulty coefficient to healthy coefficients λ and energy ratio of faulty coefficient to healthy coefficients φ.

$$\lambda = \frac{\sqrt{\sum_{m=1}^{N}(D(m) - D_{\text{mean}}(m))^2}}{\sqrt{\sum_{m=1}^{N}(D_h(m) - D_{h\text{mean}}(m))^2}} \tag{28}$$

$$\varphi = \frac{\sum_{m=0}^{N-1}|D(m)|^2}{\sum_{m=0}^{N-1}|D_h(m)|^2} \tag{29}$$

These parameters have also been used to indicate the fault severity.

3. Experimental setup & bearing fault frequencies

The experimental setup is shown in Fig. 6. The name plate details of the induction motor taken are given in Table 1. The machine was made to run via 3 phase auto transformer. This motor is mechanically loaded to obtain current samples at the time of healthy as well as faulty conditions. The data-acquisition system (NI MY DAQ) along with the current sensor LEM LA55P is used to take the stator current under both conditions. The sampling frequency is taken as 10 KHz. The sensed stator current from DAQ is processed to MATLAB for testing the algorithm practically. In the present experiment, SKF 6206ZZ single row deep grove is used as test bearing. The test bearing 6206ZZ is mounted on the shaft at driving end. The specifications of the bearing are: PD = 1.83 in., BD = 0.375 in., $n = 9$ and $\emptyset = 0^0$. The fault frequencies calculated using (1)–(5) for the above test machine are shown in Table 2.

Fig. 6. Experimental setup for bearing fault detection.

Table 2
Bearing fault frequencies.

	No-load frequencies (Hz)				Full-load (12.73 N-M) frequencies (Hz)			
	f_{out}	f_{inn}	f_{ball}	f_{cage}	f_{out}	f_{inn}	f_{ball}	f_{cage}
f_r	24.8	24.8	24.8	24.8	23.9	23.9	23.9	23.9
$m = 1$	138.8	184.6	108	70	135	179.6	106	64.4
$m = 2$	227.7	319.2	166	80	221	309.3	161.8	78.8
$m = -1$	38.8	84.6	8	35	35	79.6	6	35.5
$m = -2$	127.7	219.2	66	20	121	209.3	61.8	21.8

4. Results & discussion

In this section, simulation and experimental result of bearing faults detection in 3 phase induction motor has been presented. The flow graph of proposed topology is shown in Fig. 7. First the stator current is taken from data acquisition system and is processed for constant frequency checking. If it has constant frequency, then the current is used to design the Wiener filter coefficients for first time and in the next it is processed for noise cancellation. Otherwise, stator current is sensed again until constant frequency. Afterwards, the noise cancelled stator current is decomposed into approximated and detailed coefficients using wavelet analysis and power spectral density of the each coefficient is computed. The PSD of the required level coefficients are used to calculate the fault indexing parameters to estimate fault severity.
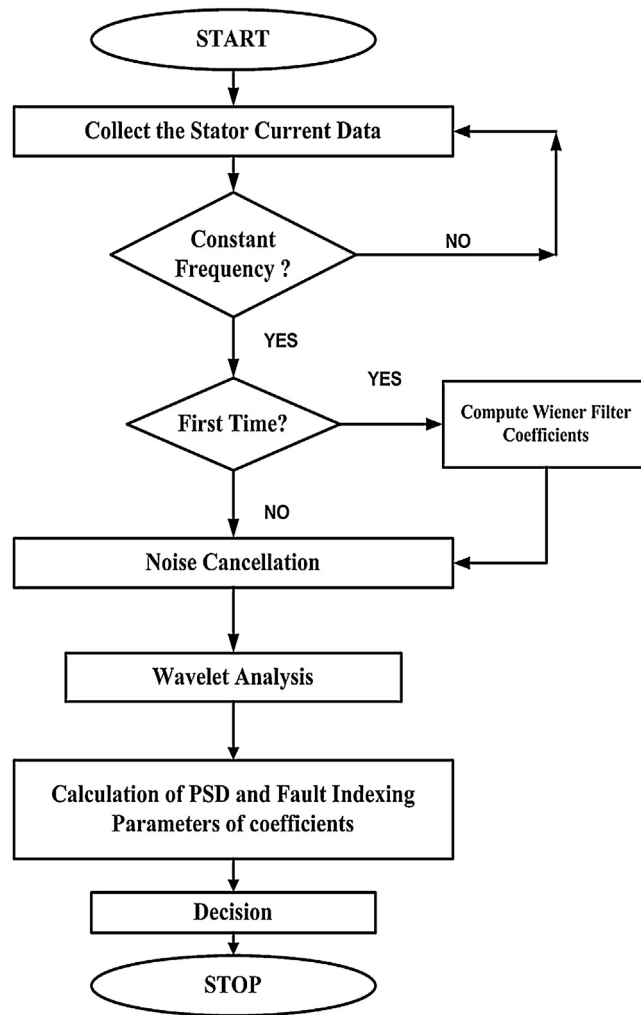
Fig. 7. Flow graph of proposed fault detection topology.

4.1. Simulation results

In this simulation work, the pre fault components of stator current is modeled using (6) with fundamental frequency 50 Hz and its 5th, 7th, and 11th harmonic components of 250 Hz, 350 Hz and 550 Hz frequencies respectively. The sensor and EMI noise is modeled by means of white Gaussian noise (WGN) with a less signal to noise ratio (SNR). The Wiener filter is designed using (18) with order $p = 2000$ and trained with a wide range of fault frequencies.

4.1.1. FFT analysis

In this, the FFT analysis of healthy stator current with and without noise cancellation is performed and compared with faulty condition of the bearing. The bearing fault frequencies for the single point defect is taken from Table 2 and introduced into the stator current to test the filter performance. The generalized roughness fault is tested with different fault severities.

The healthy stator current before and after noise cancellation is shown in Fig. 8(a) & (b) respectively. The current spectrum after noise cancellation under healthy condition shows that, a minimum noise floor is maintained due to the performance of the filter coefficients. This noise floor will become severe especially at incipient stage of the fault.
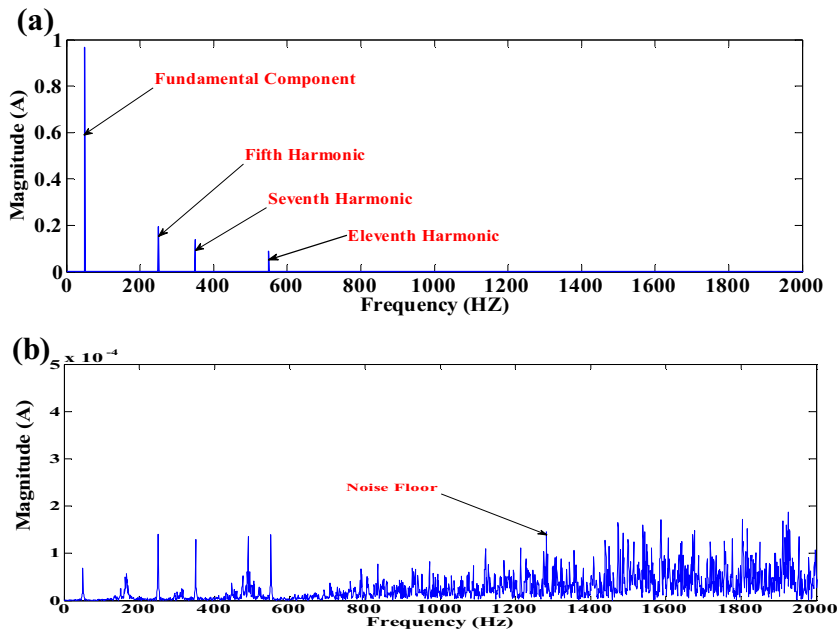
Fig. 8. Healthy stator current spectrum (a) before noise cancellation (b) after noise cancellation.

4.1.1.1. Single point defect. FFT analysis of bearing fault after noise cancellation with single point defect type is performed under no load case in Table 2. The fault frequencies of outer race, inner race, cage fault and ball defects are introduced into the stator current one after other with different magnitudes and extracted from current spectrum by noise cancellation as shown in Fig. 9(a)–d). It shows that, the FFT analysis have good performance with less value of noise floor for severe faults. At nascent stage of fault, the noise floor dominates fault component. This is the major issue in FFT analysis especially at early stage of the fault.

4.1.1.2. Generalized roughness. Estimation of non cyclic (Generalized roughness) fault using FFT analysis has a limitation that, these faults does not impose any characteristic fault frequencies into stator current spectrum. These faults will impose broad band and unpredictable frequencies into stator current. Therefore, in this section fault frequencies with random values are introduced with different magnitudes to test the proposed method for various fault severities. The fault magnitudes 0.1%, 1% and 5% are used for testing. FFT analysis of stator current spectrum for generalized fault after noise cancellation is shown in Fig. 10(a)–(c). These results are evident that the FFT analysis is suitable for the frequencies which are very far from the healthy components and have some resolution problems for the frequencies nearer to healthy components like fundamental and harmonics. Fig. 10(b) &(c) shows that, the noise floor dominates the fault component especially at the nascent stage of fault. This problem can be overcome by DWT analysis, which is presented in the next section.

4.1.2. DWT analysis

In this section, the wavelet transform based noise cancellation is performed by Daubechies wavelet function of family 8(db8) and bearing fault signal $b(n)$ is decomposed into level 8 using Eq. (27). Afterward, the approximation and detail coefficients at the level 8 are taken and performed the two criteria proposed in this paper. The ratios of standard deviation λ and energy φ are calculated and compared with the ratios of PSD values. The decomposition of healthy stator current and cage fault after noise cancellation are shown in Figs. 11–12. From Figs. 11–12 it is observed that, direct visualization of wavelet coefficients does not give any information regarding fault existence and its severity. Therefore, the fault indexing based fault estimation is presented in the following. Fig. 13 shows the bar graphs of fault indexing parameters for 4 categories of faults with different magnitudes. The fault frequencies with different magnitudes visually, 0.1%, 1% and 5% are introduced into stator current and examined using proposed method of bearing fault detection. For incipient stage fault i.e. fault with 0.1% magnitude has less indication in both parameters.
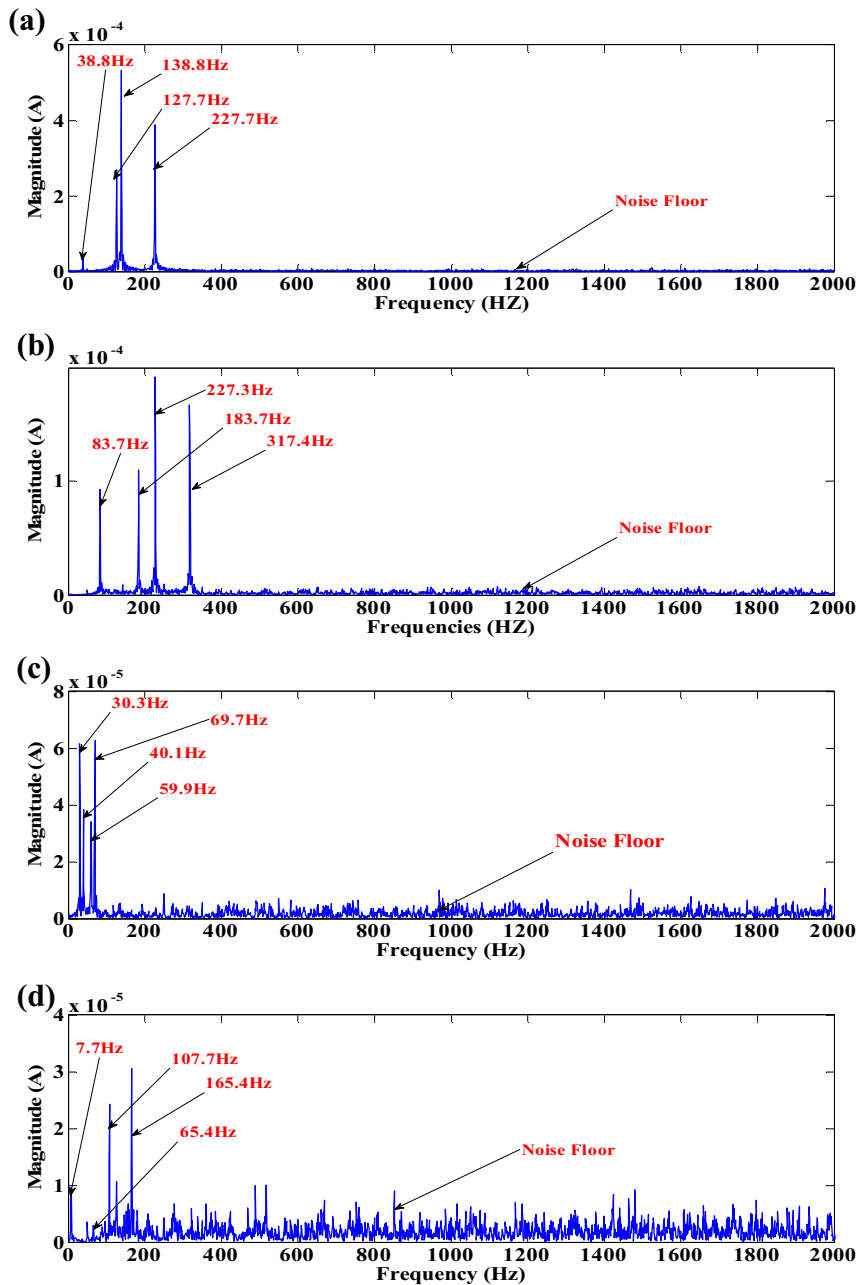
Fig. 9. Stator current after noise cancellation. (a) Outer race (b) inner race (c) cage fault (d) ball defect.

This is due to domination of noise after Wiener filtering. Direct calculation of fault indexing parameters will have poor resolution and have less information regarding fault especially at early stage. Therefore, the power spectral density based fault indexing parameter calculation is proposed and presented in the following.

The power spectral density based fault indexing parameters are shown in Fig. 14. The power spectral density has elevating the wavelet coefficients and fault indexing parameters. Consequently, the indication of fault indexing parameters is raised and gives clear information regarding fault especially at early stage (0.1%). The bar graphs in Fig. 14(a) & (d) are raised compared to Fig. 13(a) & (d). This shows the importance of power spectral density in wavelet decomposition. In the similar way, the generalized roughness fault with same variations in the magnitude (0.1%, 1%, and 5%) is examined with proposed topology and shown in Fig. 15. From this figure it is observed that, the parameter
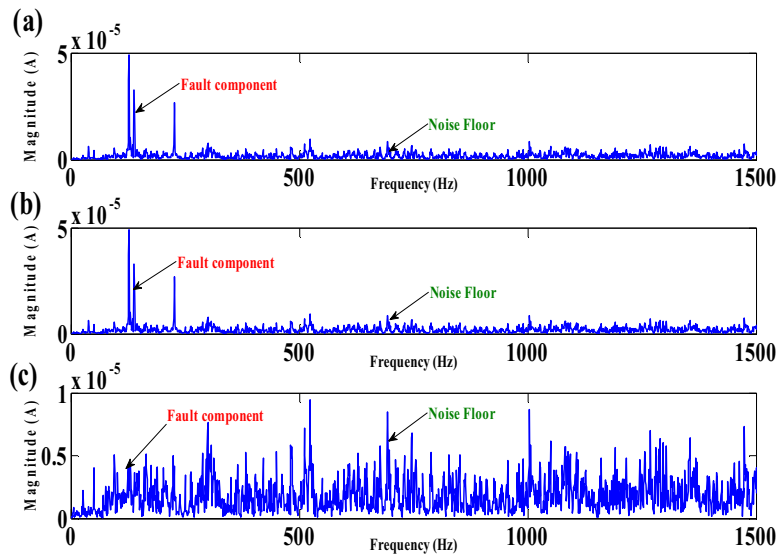
Fig. 10. FFT analysis of stator current with different magnitude, (a) with 5% fault magnitude, (b) with 1% fault magnitude and (c) 0.1% fault magnitude.
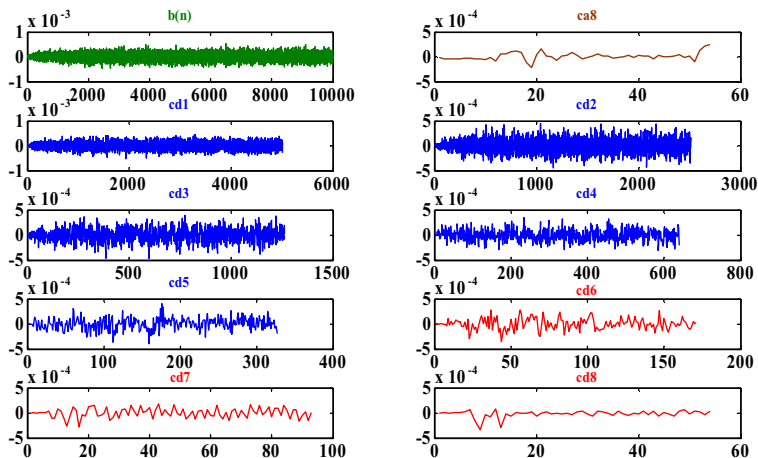

Fig. 11. Wavelet decomposition of healthy signal after noise cancellation.

SD has shown good variations in PSD based calculation whereas the parameter energy will remain unaffected even after PSD. The same will be examined using experimental setup proposed in Section 3 and the results are presented in following sub section.

4.2. Experimental results

In the experimental arrangement of bearing fault detection topology, the stator current is taken from induction machine under healthy condition of the bearing using current transducer and processed for noise cancellation by NI MYDAC. The stator current is sampled at a frequency of 10 kHz and normalized to process in MATLAB programming. Afterwards the stator current is processed for noise cancellation using Wiener filter coefficients and decomposed into 8 levels using DWT decomposition. The wavelet coefficients are used to calculate the fault indexing parameters using without power spectral density (PSD). After that for with PSD case, the decomposed DWT coefficients are processed for power spectral density calculation and then used to calculate the fault indexing parameters. These values of fault indexing parameter using with and without PSD are saved for calculation of fault ratios proposed in previous section.
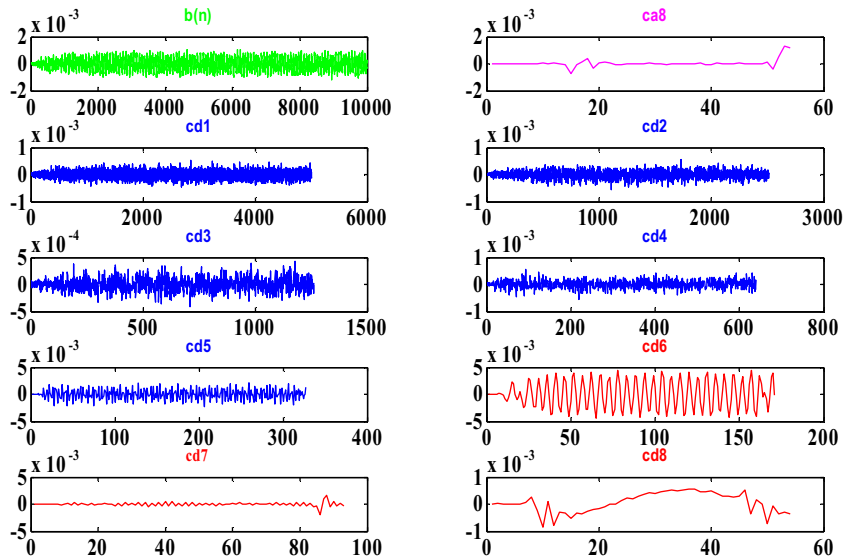
Fig. 12. Wavelet decomposition of outer race fault after noise cancellation.
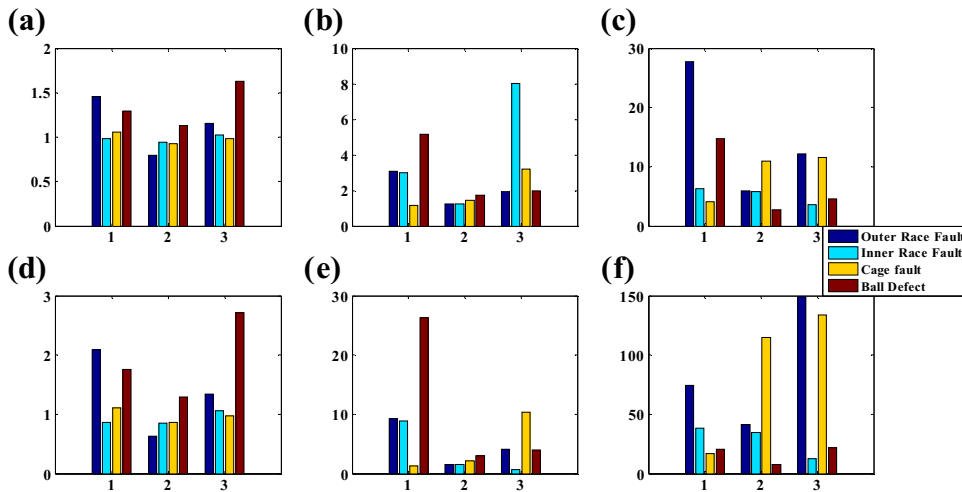

Fig. 13. Fault indexing parameters without PSD (1# CD6, 2# CD7 and 3# CD8). (a) SD of 0.1% fault, (b) SD of 1% fault, (c) SD of 5% fault, (d) energy of 0.1% fault, (e) energy of 1% fault and (f) energy of 5% fault.

Now to test the proposed algorithm for bearing fault, the faulty bearings (outer race, cage and generalized roughness) are inserted into the machine one after other and repeat the entire process to obtain fault indexing parameters for each case. The ratios for faulty to healthy parameters are plotted in Fig. 16. In Fig. 16 the impact of outer race fault is less compared to cage fault. That means, the outer race fault is at early stage and cage fault is at severe stage. The standard deviation and energy in Fig. 16(a) & (b) for both the faults shows the standard deviation has poor performance compared to energy. Especially for outer race fault, the standard deviation gives poor indication and is difficult to estimate the fault. In the case of energy parameter all the coefficients of DWT have good indication and it is easy to predict the fault component at early stage. But after calculation of power spectral density for the wavelet coefficients, the indications for incipient fault are greatly improved in both the parameters and have a good sign for fault as shown in Fig. 16(c)–(d). Therefore, the power spectral density of wavelet coefficients greatly highlights the fault indication in both the parameters for all categories of fault.

In the case of generalized roughness fault, the ratios of fault indexing parameters are shown in Fig. 17. In this case also, the fault indexing parameters are greatly improved using power spectral density as mentioned in simulation part.
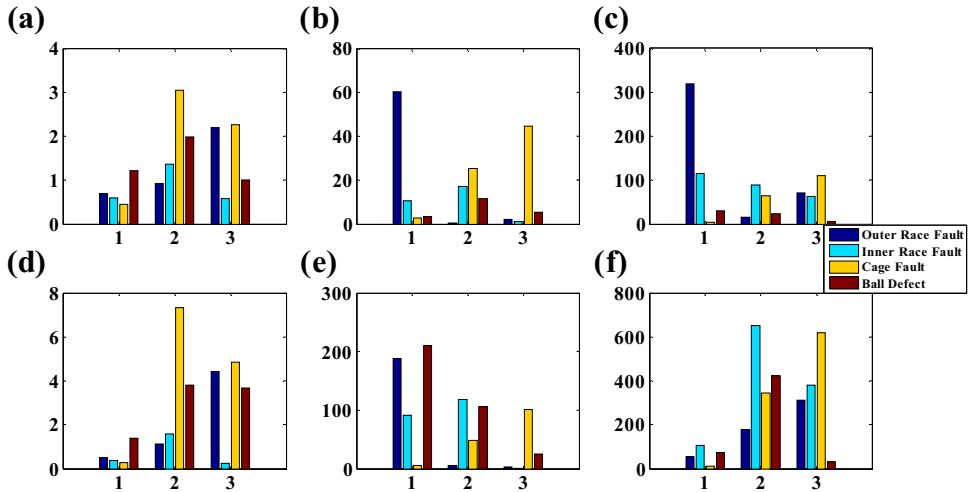
Fig. 14. Fault indexing parameters with PSD (1# CD6, 2# CD7 and 3# CD8). (a) SD of 0.1% fault, (b) SD of 1% fault, (c) SD of 5% fault, (d) energy of 0.1% fault, (e) energy of 1% fault and (f) energy of 5% fault.
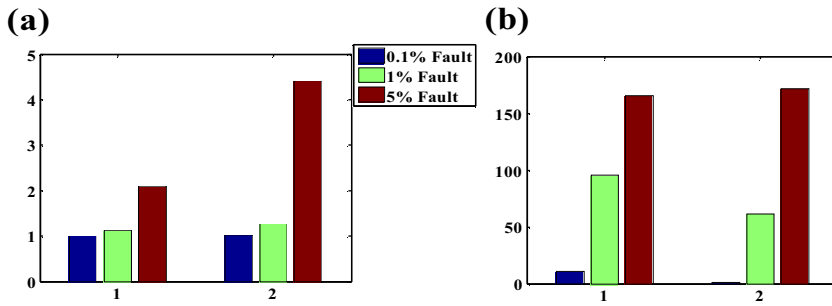
Fig. 15. Fault index parameters for generalized roughness fault with different fault severities (1# SD, 2# energy) (a) without PSD and (b) with PSD.
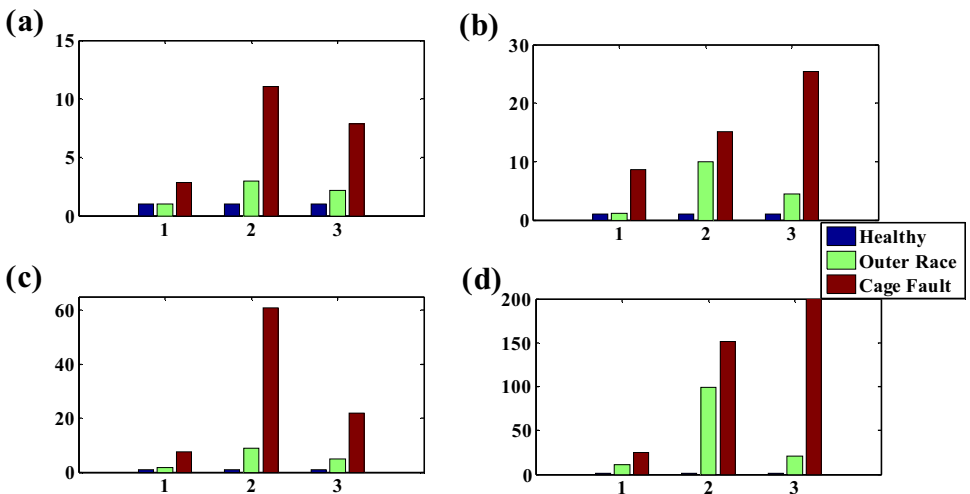
Fig. 16. Experimental fault indexing parameters using with & without power spectral density (1# CD6, 2# CD7 and 3# CD8). (a) SD without PSD, (b) energy without PSD, (c) SD with PSD and (d) energy with PSD.
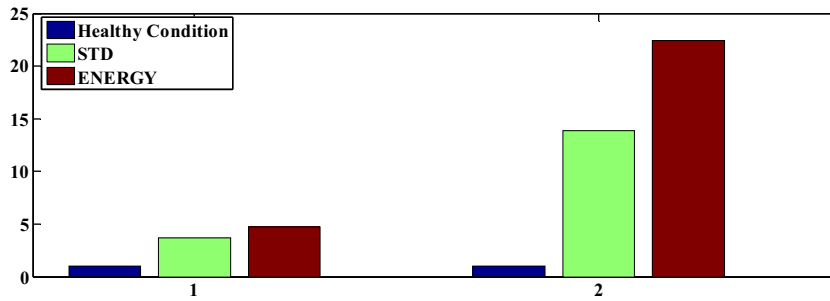
Fig. 17. Experimental fault indexing parameters for generalized roughness fault using with & without power spectral density (1# without PSD, 2# with PSD).

The standard deviation and energy of with and without PSD are shown in Fig. 17. The parameters are greatly improved after PSD based calculation as shown in Fig. 17. Therefore, the bearing fault detection using noise cancellation with power spectral density of DWT analysis gives good results compared to conventional analysis of DWT.

5. Conclusions

This paper has presented an approach to detect the incipient state bearing faults in induction motor using stator current signature analysis via noise cancellation using DWT decomposition. The healthy components of stator current are estimated and cancelled using Wiener filter coefficients. The standard deviation and energy ratios of faulty to healthy stator current are calculated as fault index. Two types of frequency domain analysis have been presented to detect the bearing faults. DWT analysis of stator current after noise cancellation has overcome the drawbacks of the FFT analysis for early stage faults. The proposed method has shown improved performance using power spectral density based DWT analysis. The fault indexing parameters SD and energy have shown almost equal performance at severe stage of fault. At incipient stage, SD shown some good indication compared to PSD analysis. Though the SD have maintain same indication even after PSD calculation, the energy indication have raised abruptly to maximum. Therefore, the energy with PSD based fault detection has given good results compared to other. The results have confirmed the effectiveness of the proposed technique.

In Future, the effect of severe noise may be reduced by proper de-noising techniques like Wavelet De-Noising and deconvolution and the Wiener filter coefficients may be designed using better error minimization techniques.

Acknowledgement

References

Bellini, A., Immovilli, F., Rubini, R., Tassoni, C., 2008a. Diagnosis of bearing faults in induction machines by vibration or current signals: a critical comparison. In: Conf Rec. IEEE IAS Annu. Meeting, Edmonton, AB, Canada, October, pp. 1–8.

Bellini, A., Yazidi, A., Filippetti, F., Rossi, C., Capolino, G., 2008b. High frequency resolution techniques for rotor fault detection of nductionma-chines. IEEE Trans. Ind. Electron. 55 (December (12)), 4200–4209.

Blodt, M., Granjon, P., Raiso, B., Rostaing, G., 2008. Models for bearing damage detection in induction motors using stator current monitoring. IEEE Trans. Ind. Electron. 55 (April (4)), 1813–1822.

El Houssin, El Bouchikhi, Choqueuse, Vincent, El Hachemi Benbouzid, Mohamed, 2013. Current frequency spectral subtraction and its contribution to induction machines bearings condition monitoring. IEEE Trans. Energy Convers. 28 (March (1)), 135–144.

Eren, L., Devaney, M.J., 2004. Bearing damage detection via wavelet packet decomposition of the stator current. IEEE Trans. Instrum. Meas. 53 (April (2)), 431–436.

Filippetti, F., Franceschini, G., Tassoni, C., 1995. Neural networks aided on-line diagnostics of induction motor rotor faults. IEEE Trans. Ind. Appl. 31 (July/August (4)), 892–899.

Frosini, L., Bassi, E., 2010. Stator current and motor efficiency as indicators for different types of bearing faults in induction motors. IEEE Trans. Ind. Electron. 57 (January (1)), 244–251.

Garcia-Perez, A., Romero-Troncoso, R.J., Cabal-Yepez, E., Osornio-Rios, R.A., 2011. The application of high-resolution spectral analysis for identifying multiple combined faults in induction motors. IEEE Trans. Ind. Electron. 58 (May (5)), 2002–2010.

Hedayati Kia, S., Henao, H., Capolino, Gérard-André, 2009. Diagnosis of broken-bar fault in induction machines using discrete wavelet transform without slip estimation. IEEE Trans. Ind. Appl. 45 (July/August (4)), 1395–1404.

Jung, J.-H., Lee, J.-J., Kwon, B.-H., 2006. Online diagnosis of induction motors using MCSA. IEEE Trans. Ind. Electron. 53 (December (6)), 1842–1852.

Kia, S.H., Henao, H., Capolino, G.-A., 2007. A high-resolution frequency estimation method for three-phase induction machine fault detection. IEEE Trans. Ind. Electron. 54 (August (4)), 2305–2314.

Kim, B.S., Lee, S.H., Lee, M.G., Ni, J., Song, J.Y., Lee, C.W., 2007. A comparative study on damage detection in speed-up and coast-down process of grinding spindle-typed rotor-bearing system. J. Mater. Process. Technol. 187/188 (June), 30–36.

Kim, Y.H., Youn, Y.W., Hwang, D.H., Sun, J.H., Kang, D.S., 2013. High-resolution parameter estimation method to identify broken rotor bar faults in induction motors. IEEE Trans. Ind. Electron. 60 (September (9)), 4103–4117.

Kompella, K.C. Deekshit, Rao, M.V., Rao, R.S., Sreenivasu, R., 2013. Estimation of nascent stage bearing faults of induction motor by stator current signature using adaptive signal processing. In: Proc. IEEE INDICON, December, pp. 1–5.

Lau, E.C.C., Ngan, H.W., 2010. Detection of motor bearing outer raceway defect by wavelet packet transformed motor current signature analysis. IEEE Trans. Instrum. Meas. 59 (October (10)), 2683–2690.

Liu, Jie, Wang, Wilson, Golnaraghi, Farid, 2008. An extended wavelet spectrum for bearing fault diagnostics. IEEE Trans. Instrum. Meas. 57 (December (12)), 2801–2812.

Luo, J., Yu, D., Liang, M., 2013. A kurtosis-guided adaptive demodulation technique for bearing fault detection based on tunable-Q wavelet transform. J. Meas. Sci. Technol. 24 (May (5)), 1–11.

Obaid, R.R., Habetler, T.G., Stack, J.R., 2003. Stator current analysis for bearing damage detection in induction motors. In: Proc. 4th IEEE SDEMPED, August, pp. 182–187.

Report on large motor reliability survey of industrial and commercial installations—part I., 1985a. IEEE Trans. Ind. Appl. IA-21 (July/August (4)), 853–864.

Report on large motor reliability survey of industrial and commercial installations—part II., 1985b. IEEE Trans. Ind. Appl. IA-21 (July/August (4)), 865–872.

Schoen, R.R., Habetler, T.G., Kamran, F., Bartheld, R.G., 1995. Motor bearing damage detection using stator current monitoring. IEEE Trans. Ind. Appl. 31 (November/December (6)), 1274–1279.

Soualhi, Abdenour, Medjaher, Kamal, Zerhouni, Noureddine, 2015. Bearing health monitoring based on Hilbert–Huang transform, support vector machine, and regression. IEEE Trans. Instrum. Meas. 64 (1), 52–62.

Stack, J.R., Harley, R.G., Habetler, T.G., 2004a. An amplitude modulation detector for fault diagnosis in rolling element bearings. IEEE Trans. Ind. Electron. 51 (May (5)), 1097–1102.

Stack, J.R., Habetler, T.G., Harley, R.G., 2004b. Bearing fault detection via autoregressive stator current modeling. IEEE Trans. Ind. Appl. 40 (May/June (3)), 740–747.

Stack, J.R., Habetler, T.G., Harley, R.G., 2004c. Fault classification and fault signature production for rolling element bearings in electric machines. IEEE Trans. Ind. Appl. 40 (May/June (40)), 735–739.

Stack, J.R., Habetler, T.G., Harley, R.G., 2006. Fault-signature modeling and detection of inner-race bearing faults. IEEE Trans. Ind. Appl. 42 (January/February (1)), 61–68.

Sun, W., Yang, G., Chen, Q., Palazoglu, A., Feng, K., 2013. Fault diagnosis of rolling bearing based on wavelet transform and envelope spectrum correlation. J. Vib. Control 19 (April (6)), 924–941.

Vicente, Climente-Alarcon, et al., 2014. Induction motor diagnosis by advanced notch FIR filters and the Wigner–Ville distribution. IEEE Trans. on Ind. Electron 61 (August (8)), 4217–4227.

Wei, Z., Gao, J., Zhong, X., Jiang, Z., Ma, B., 2011. Incipient fault diagnosis of rolling element bearing based on wavelet packet transform and energy operator. WSEAS Trans. Syst. 10 (March (3)), 81–90.

Zhang, Pinjia, et al., 2011. A survey of condition monitoring and protection methods for medium-voltage induction motors. IEEE Trans. Ind. Appl. 47 (January (1)), 34–46.

Zhongming, Y., Wu, B., Sadeghian, A.R., 2001. Signature analysis of induction motor mechanical faults by wavelet packet decomposition. 16th Annu. IEEE Applied Power Electronics Conf. Expos. vol. 2, 1022–1029.

Zhou, Wei, Lu, Bin, Ghabetler, T., Ronald Harley, G., 2009. Incipient bearing fault detection via motor stator current noise cancellation using Wiener filter. IEEE Trans. Ind. Appl. 45 (July/August (4)), 1309–1317.

Mr. K. K. C. Deekshit is currently working towards Doctoral degree in Electrical & Electronics Engineering, JNTUK, Kakinada, A.P., India. Previously he worked for K.L.University, Guntur, India. He is currently an Assistant professor in the Department of Electrical and Electronics Engineering, PVPSIT, Kanuru, A.P, India. His current research interest includePower Electronics Induction motor drives and Signal Processing.

Dr. Venu Gopala Rao. M., FIE, MIEEE at present is Professor and Head, Department of Electrical & Electronics Engineering, PVPSIT, Kanuru, A.P., India. Previously he worked for K.L.University, Guntur. He published more than 20 papers in various National, International Conferences and Journals. His research interests accumulate in the area of Power Quality, Distribution System, High Voltage Engineering and Electrical Machines.

Dr. R. Srinivasa Rao, MIEEE at present is a Professor in Electrical and Electronics Engineering Department, Jawaharlal Nehru Technological University Kakinada, Kakinada, A.P., India. His area of interest includes electrical power distribution systems and power system operation and control.